Simulation of Emission Spectra for LH4 Ring: Intermolecular Coupling Fluctuation Effect

Pavel Heřman, David Zapletal

***Abstract*—** Photosynthesis starts with the absorption of a solar photon by one of the light-harvesting (LH) pigment-protein complexes and transferring the excitation energy to the reaction center where a charge separation is initiated. Knowledge of the microscopic structure of some photosynthetic systems and their function invokes during last twenty years long and intensive investigation of many theoretical and experimental laboratories. The geometric structure of LH complexes is known in great detail, e.g. for the LH2 and LH4 complexes of purple bacteria. Absorption and steady state fluorescence spectra of exciton states for ring molecular systems are presented. The peripheral cyclic antenna unit LH4 of the bacterial photosystem from purple bacteria can be modeled by such system. The cumulant-expansion method of Mukamel et al. is used for the calculation of spectral responses of the system with exciton-phonon coupling. Dynamic disorder, interaction with a bath, in Markovian approximation simultaneously with uncorrelated static disorder in transfer integrals are taking into account in our simulations. We compare calculated absorption and steady state fluorescence spectra for LH4 ring obtained within the full Hamiltonian model with our previous results within nearest neighbour approximation model for uncorrelated static disorder in transfer integrals. All calculations were done in software package *Mathematica*.

***Keywords*—**LH4, absorption and fluorescence spectrum, static and dynamic disorder, exciton states, *Mathematica*

I. Introduction

In the process of photosynthesis (in plants, bacteria, and blue-green algae), solar energy is used to split water and produce oxygen molecules, protons and electrons. Photosynthesis starts with the absorption of a solar photon which is is absorbed by a complex system of membrane-associated pigment-proteins (light-harvesting (LH) antenna) and absorbed energy is efficiently transferred to a reaction center (RC), where it is converted into a chemical energy [1]. These initial ultrafast events have been extensively investigated. Knowledge of the microscopic structure of some photosynthetic systems, e.g., photosynthetic systems of purple bacteria, invokes during last twenty years long and intensive effort of many theoretical and experimental laboratories. Our interest is mainly focused on first (light) stage of photosynthesis in purple bacteria.

The antenna systems of photosynthetic units from purple bacteria are formed by ring units LH1, LH2, LH3, and LH4. Their geometric structures are known in great detail from X-ray crystallography. The general organization of above mentioned light-harvesting complexes is the same: identical subunits are repeated cyclically in such a way that a ring-shaped structure is formed. However the symmetries of these rings are different.

The core antenna LH1 contained in purple bacteria such as *Rhodopseudomonas palustris* consists of approximately 16 structural subunits in which two bacteriochlorophyll *a* (BChl-*a*) molecules are noncovalently attached to pairs of transmembrane polypeptides. These subunits are arranged in a ringlike structure which surround the RC. In the near infrared LH1 absorbs at 870 nm. More about crystal structure of this core complex is possible to find e.g. in [2].

Crystal structure of LH2 complex contained in purple bacterium Rhodopseudomonas acidophila in high resolution was first described by McDermott et al. [3] in 1995, then further e.g. by Papiz et al. [4] in 2003. The bacteriochlorophyll (BChl) molecules are organized in two concentric rings. One ring features a group of nine well-separated BChl molecules (B800) with absorption band at about 800 nm. The other ring consists of eighteen closely packed BChl molecules (B850) absorbing around 850 nm. LH2 complexes from other purple bacteria have analogous ring structure.

Some bacteria express also other types of complexes such as the B800-820 LH3 complex (*Rhodopseudomonas acidophila* strain 7050) or the LH4 complex (*Rhodopseudomonas palustris*). LH3 complex like LH2 one is usually nonameric but LH4 one is octameric. While the B850 dipole moments in LH2 ring have tangential arrangement, in the LH4 ring they are oriented more radially. Mutual interactions of the nearest neighbour BChls in LH4 are approximately two times smaller in comparison with LH2 and have opposite sign. The other

Manuscript received January 10, 2014.

This work was supported in part by the Faculty of Science, University of Hradec Králové (project of specific research No. 2112/2013 - P. Heřman).

P. Heřman is with the Department of Physics, Faculty of Science, University of Hradec Králové, Rokitanského 62, 50003 Hradec Králové, Czech Republic (e-mail: pavel.herman@uhk.cz).

D. Zapletal is with the Institute of Mathematics and Quantitative Methods, Faculty of Economics and Administration, University of Pardubice, Studentská 95, 53210 Pardubice, Czech Republic (e-mail: david.zapletal@upce.cz).

difference is the presence of an additional BChl ring in LH4 complex [5]. Different arrangements manifest themselves in different optical properties. At this article we mainly focus on LH4 complex.

The intermolecular distances under 1 nm determine strong exciton couplings between corresponding pigments. Due to the strong interaction between BChl molecules, an extended Frenkel exciton states model is considered in our theoretical approach. Despite intensive study of bacterial antenna systems, e.g. [3]–[6], the precise role of the protein moiety for governing the dynamics of the excited states is still under debate. At room temperature the solvent and protein environment fluctuates with characteristic time scales ranging from femtoseconds to nanoseconds. The simplest approach is to substitute fast fluctuations by dynamic disorder and slow fluctuation by static disorder.

In our previous papers we presented results of simulations doing within the nearest neighbour approximation model. In several steps we extended the former investigations of static disorder effect on the anisotropy of fluorescence made by Kumble and Hochstrasser [7] and Nagarajan et al. [8]–[10] for LH2 ring. After studying the influence of diagonal dynamic disorder for simple systems (dimer, trimer) [11]–[13], we added this effect into our model of LH2 ring by using a quantum master equation in Markovian and non-Markovian limits [14]–[16]. We also studied influence of four types of uncorrelated static disorder [17], [18] (Gaussian disorder in local excitation energies, Gaussian disorder in transfer integrals, Gaussian disorder in radial positions of BChls and Gaussian disorder in angular positions of BChls on the ring). Influence of correlated static disorder, namely an elliptical deformation of the ring, was also taken into account [14]. We also investigated the time dependence of fluorescence anisotropy for the LH4 ring with different types of uncorrelated static disorder [16], [19].

Recently we have focused on the modeling of absorption and steady state fluorescence spectra. Our results for LH2 and LH4 rings within the nearest neighbour Hamiltonian model have been presented in [20]–[25]. The results for LH2 ring within full Hamiltonian model have been published in [26], [27].

Present paper is the extension of our contribution presented on WSEAS conference AMATH'13. Main goal of the paper is the comparison of the results for LH4 ring calculated within full Hamiltonian model with the previous results calculated within the nearest neighbour approximation model. The rest of the paper is organized as follows. Section 2 introduces the ring model with the static disorder and dynamic disorder (interaction with phonon bath) and the cumulant expansion method, which is used for the calculation of spectral responses of the system with exciton-phonon coupling. Computational point of view is mentioned in Section 3. The presented results of our simulations and used units and parameters could be found in Section 4, in Section 5 some conclusions are drawn.

II. Physical model

We assume that only one excitation is present on the ring after an impulsive excitation. The Hamiltonian of an exciton in the ideal ring coupled to a bath of harmonic oscillators reads

$$H^0 = H^0_{\rm ex} + H_{\rm ph} + H_{\rm ex--ph}. \tag{1}$$

Here the first term,

$$H^0_{\rm ex} = \sum_{m,n(m\neq n)} J_{mn} a^\dagger_m a_n, \tag{2}$$

corresponds to an exciton, e.g. the system without any disorder. The operator $a^\dagger_m$ (a_m) creates (annihilates) an exciton at site m, J_{mn} (for $m \neq n$) is the so-called transfer integral between sites m and n. The second term,

$$H_{\rm ph} = \sum_q \hbar\omega_q b^\dagger_q b_q, \tag{3}$$

represents phonon bath in harmonic approximation (the phonon creation and annihilation operators are denoted by $b^\dagger_q$ and b_q, respectively). Last term in (1),

$$H_{\rm ex-ph} = \frac{1}{\sqrt{N}} \sum_m \sum_q G^m_q \hbar\omega_q a^\dagger_m a_m (b^\dagger_q + b_q), \tag{4}$$

describes exciton-phonon interaction which is assumed to be site-diagonal and linear in the bath coordinates (the term G^m_q denotes the exciton-phonon coupling constant).

Inside one ring the pure exciton Hamiltonian can be diagonalized using the wave vector representation with corresponding delocalized "Bloch" states α and energies E_α. Considering homogeneous case with only the nearest neighbour transfer matrix elements

$$J_{mn} = J_0(\delta_{m,n+1} + \delta_{m,n-1}) \tag{5}$$

and using Fourier transformed excitonic operators (Bloch representation)

$$a_\alpha = \sum_n a_n {\rm e}^{{\rm i}\alpha n}, \tag{6}$$

where

$$\alpha = \frac{2\pi}{N} l,\ l = 0, \pm 1, \ldots, \pm\frac{N}{2}, \tag{7}$$

the simplest exciton Hamiltonian in α - representation reads

$$H^0_{\rm ex} = \sum_\alpha E_\alpha a^\dagger_\alpha a_\alpha, \tag{8}$$

with

$$E_\alpha = -2J_0 \cos\alpha \tag{9}$$

(see Fig. 1 - left column). In case of the full Hamiltonian model (dipole-dipole approximation), energetic

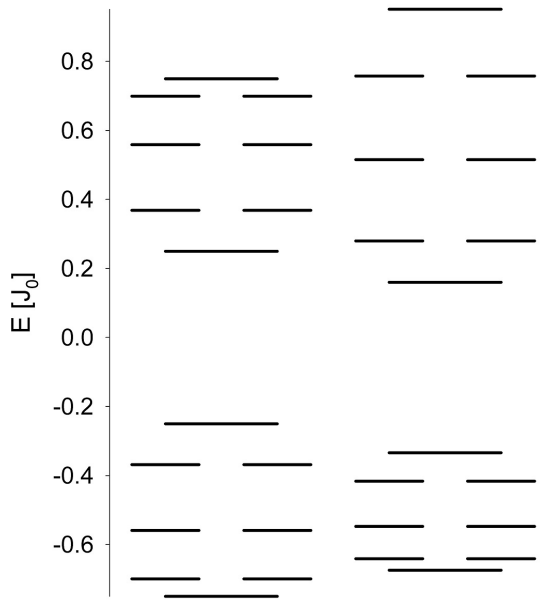

Fig. 1. Energetic band structure of the ring from LH4 (left column - the nearest neighbour approximation model, right column - full Hamiltonian model.

band structure slightly differs (Fig. 1 - right column). Differences of energies in lower part of the band are smaller and in upper part of the band are larger in comparison with the nearest neighbour approximation model.

Influence of uncorrelated static disorder is modeled by the local excitation energy fluctuations $\delta\varepsilon_n$ with Gaussian distribution and standard deviation Δ

$$H_{\mathrm{s}} = \sum_n \delta\varepsilon_n a_n^\dagger a_n. \tag{10}$$

The Hamiltonian H_{s} of the uncorrelated static disorder adds to the Hamiltonian H_{ex}^0.

The cumulant-expansion method of Mukamel et al. [28], [29] is used for the calculation of spectral responses of the system with exciton-phonon coupling. Absorption $OD(\omega)$ and steady-state fluorescence $FL(\omega)$ spectrum can be expressed as

$$OD(\omega) = \omega \sum_\alpha d_\alpha^2 \times \\ \times \mathrm{Re}\int_0^\infty dt \mathrm{e}^{\mathrm{i}(\omega-\omega_\alpha)t - g_{\alpha\alpha\alpha\alpha}(t) - R_{\alpha\alpha\alpha\alpha}t}, \tag{11}$$

$$FL(\omega) = \omega \sum_\alpha P_\alpha d_\alpha^2 \times \\ \times \mathrm{Re}\int_0^\infty dt \mathrm{e}^{\mathrm{i}(\omega-\omega_\alpha)t + \mathrm{i}\lambda_{\alpha\alpha\alpha\alpha}t - g^*_{\alpha\alpha\alpha\alpha}(t) - R_{\alpha\alpha\alpha\alpha}t}. \tag{12}$$

Here

$$\vec{d_\alpha} = \sum_n c_n^\alpha \vec{d_n} \tag{13}$$

is the transition dipole moment of eigenstate α, c_n^α are the expansion coefficients of the eigenstate α in site representation and P_α is the steady state population of the eigenstate α. The inverse lifetime of exciton state $R_{\alpha\alpha\alpha\alpha}$ is given by the elements of Redfield tensor $R_{\alpha\beta\gamma\delta}$ [30]. It is a sum of the relaxation rates between exciton states,

$$R_{\alpha\alpha\alpha\alpha} = -\sum_{\beta\neq\alpha} R_{\beta\beta\alpha\alpha}. \tag{14}$$

The g-function and λ-values in (12) are given by

$$g_{\alpha\beta\gamma\delta} = -\int_{-\infty}^{\infty} \frac{d\omega}{2\pi\omega^2} C_{\alpha\beta\gamma\delta}(\omega) \times \\ \times \left[\coth\frac{\omega}{2k_{\mathrm{B}}T}(\cos\omega t - 1) - \mathrm{i}(\sin\omega t - \omega t)\right], \tag{15}$$

$$\lambda_{\alpha\beta\gamma\delta} = -\lim_{t\to\infty}\frac{d}{dt}\mathrm{Im}\{g_{\alpha\beta\gamma\delta}(t)\} = \\ = \int_{-\infty}^{\infty}\frac{d\omega}{2\pi\omega} C_{\alpha\beta\gamma\delta}(\omega). \tag{16}$$

The matrix of the spectral densities $C_{\alpha\beta\gamma\delta}(\omega)$ in the eigenstate (exciton) representation reflects one-exciton states coupling to the manifold of nuclear modes. In what follows only a diagonal exciton phonon interaction in site representation is used (see (1)), i.e., only fluctuations of the pigment site energies are assumed and the restriction to the completely uncorrelated dynamical disorder is applied.

In such case each site (i.e. each chromophore) has its own bath completely uncoupled from the baths of the other sites. Furthermore it is assumed that these baths have identical properties [15], [31], [32]

$$C_{mnm'n'}(\omega) = \delta_{mn}\delta_{mm'}\delta_{nn'}C(\omega). \tag{17}$$

After transformation to the exciton representation we have

$$C_{\alpha\beta\gamma\delta}(\omega) = \sum_n c_n^\alpha c_n^\beta c_n^\gamma c_n^\delta C(\omega). \tag{18}$$

Various models of spectral density of the bath are used in literature [33]–[35]. In our present investigation we have used the model of Kühn and May [34]

$$C(\omega) = \Theta(\omega) j_0 \frac{\omega^2}{2\omega_c^3}\mathrm{e}^{-\omega/\omega_c} \tag{19}$$

which has its maximum at $2\omega_c$.

Localization of the exciton states contributing to the steady state fluorescence spectrum can be characterized by the thermally averaged participation ratio $\langle PR\rangle$, which is given by

$$\langle PR\rangle = \frac{\sum_\alpha PR_\alpha\ \mathrm{e}^{-\frac{E_\alpha}{k_B T}}}{\sum_\alpha \mathrm{e}^{-\frac{E_\alpha}{k_B T}}}, \tag{20}$$

where

$$PR_\alpha = \sum_{n=1}^N |c_n^\alpha|^4. \tag{21}$$

III. Computational point of view

To have steady state fluorescence spectrum $FL(\omega)$ and absorption spectrum $OD(\omega)$, it is necessary to calculate single ring $FL(\omega)$ spectrum and $OD(\omega)$ spectrum for large number of different static disorder realizations created by random number generator. Finally these results have to be averaged over all realizations of static disorder. Time evolution of exciton density matrix has to be calculate also for each realization of static disorder. That is why it was necessary to put through numerical integrations for each realization of static disorder (see (12)).

For the most of our calculations the software package *Mathematica* [36] was used. This package is very convenient not only for symbolic calculations [37] which are needed for expression of all required quantities, but it can be used also for numerical ones [38]. That is why the software package *Mathematica* was used by us as for symbolic calculations as for numerical integrations and also for final averaging of results over all realizations of static disorder.

IV. Results

Above mentioned type of uncorrelated static disorder, e.g. fluctuations of transfer integrals δJ_{mn}, has been taken into account in our simulations simultaneously with diagonal dynamic disorder in Markovian approximation. Resulting absorption $OD(\omega)$ and steady state fluorescence $FL(\omega)$ spectra for LH4 ring obtained within the full Hamiltonian model are compared with our previous results calculated within the nearest neighbour approximation model.

Dimensionless energies normalized to the transfer integral J_0 ($J_0 = J_{12}$ in LH2 ring) have been used. Estimation of J_0 varies in literature between $250\ \mathrm{cm}^{-1}$ and $400\ \mathrm{cm}^{-1}$. The transfer integrals in LH4 ring have opposite sign in comparison with LH2 ring and differ also in their absolute values. Furthermore, stronger dimerization can be found in LH4 in comparison with LH2 [5]. Therefore we have taken the values of transfer integrals in LH4 ring as follows: $J_{12}^{LH4} = -0.5 J_{12}^{LH2} = -0.5 J_0$, $J_{23}^{LH4} = 0.5 J_{12}^{LH4} = -0.25 J_0$. All our simulations of LH4 spectra have been done with the same values of $J_0 = 370$ cm^{-1} and unperturbed transition energy from the ground state $E_0 = 12280$ cm^{-1}, that we

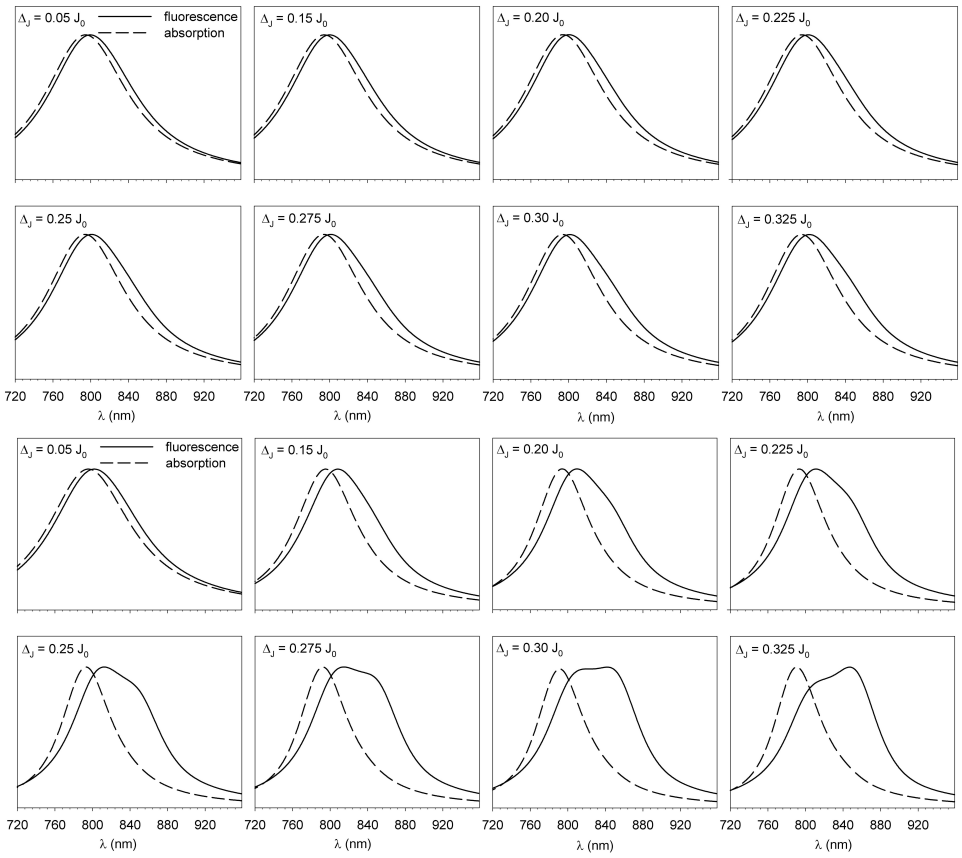

Fig. 2. Calculated fluorescence (FL) and absorpion (OD) spectra of LH4 ring averaged over 2000 realizations of static disorder in transferintegrals δJ_{mn} (room temperature $kT = 0.5\ J_0$, eight strengths $\Delta_J = 0.05,\ 0.15,\ 0.20,\ 0.225,\ 0.25,\ 0.275,\ 0.30,\ 0.325\ J_0$, full Hamiltonian model – first and second line, the nearest neighbour approximation model – third and fourth line).

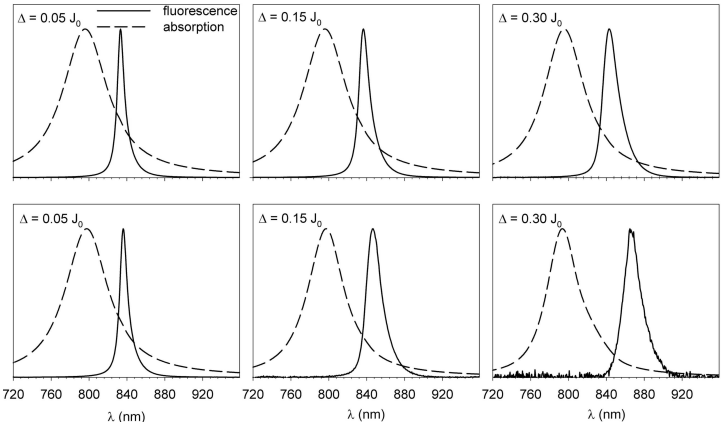

Fig. 3. Calculated fluorescence (FL) and absorpion (OD) spectra of LH4 ring averaged over 2000 realizations of static disorder in transferintegrals δJ_{mn} (low temperature $kT = 0.1\ J_0$, three strengths $\Delta_J = 0.05,\ 0.15,\ 0.30\ J_0$, full Hamiltonian model – first row, the nearest neighbour approximation model – second row).

found for LH2 ring (the nearest neighbour approximation model) [20]. The model of spectral density of Kühn and May [34] has been used in our simulations. In agreement with our previous results [17], [39] we have used $j_0 = 0.4\ J_0$ and $\omega_c = 0.212\ J_0$ (see (19)). The strengths of uncorrelated static disorder has been taken in agreement with [40]: $\Delta = 0.1,\ 0.2,\ 0.3,\ 0.4\, J_0$.

The strengths of Gaussian uncorrelated static disorder in transfer integrals Δ_J have been taken in agreement with [40], i.e. $\Delta_J \in \langle 0.05\ J_0,\ 0.3\ J_0 \rangle$. Three strengths $\Delta_J = 0.05,\ 0.15,\ 0.3\ J_0$ have been chosen for low temperature $kT = 0.1\ J_0$. Because

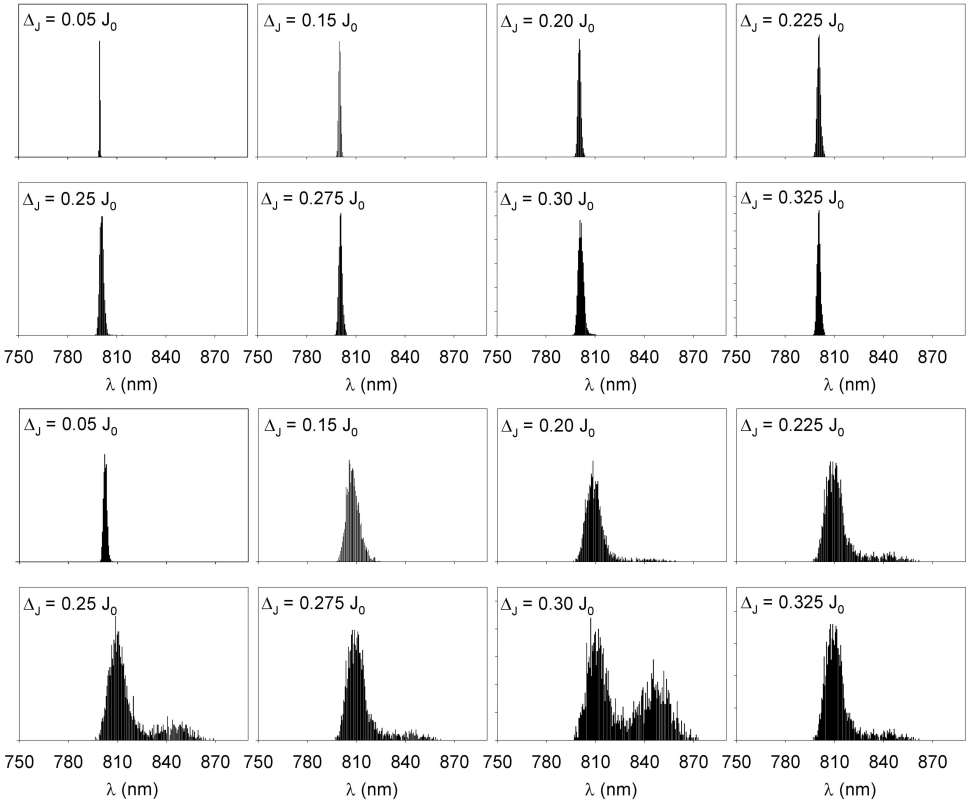

Fig. 4. Peak position distributions of calculated steady-state single ring fluorescence (FL) spectra of LH4 ring for 2000 realizations of Gaussian uncorrelated static disorder in transferintegrals δJ_{mn} (room temperature $kT = 0.5\ J_0$, eigth strengths $\Delta_J = 0.05,\ 0.15,\ 0.20,\ 0.225,\ 0.25,\ 0.275,\ 0.30,\ 0.325\ J_0$, full Hamiltonian model – first and second row, the nearest neighbour approximation model – third and fourth row).

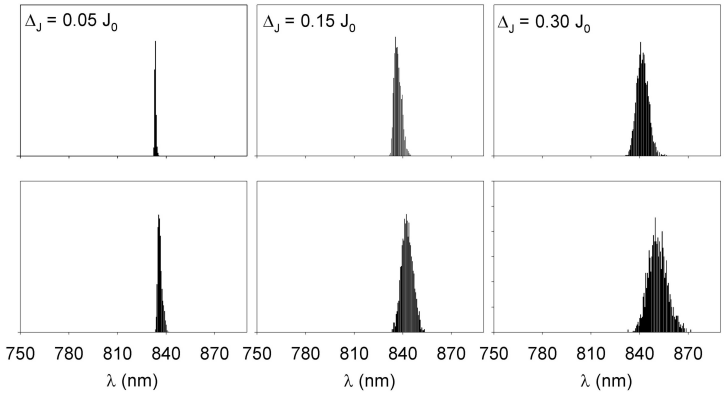

Fig. 5. Peak position distributions of calculated steady-state single ring fluorescence (FL) spectra of LH4 ring for 2000 realizations of Gaussian uncorrelated static disorder in transferintegrals δJ_{mn} (low temperature $kT = 0.1\ J_0$, three strengths $\Delta_J = 0.05,\ 0.15,\ 0.30\ J_0$, full Hamiltonian model – first row, the nearest neighbour approximation model – second row).

of fluorescence spectral line splitting in case of room temperature $kT = 0.5\ J_0$, eight strengths $\Delta_J = 0.05,\ 0.15,\ 0.2,\ 0.225,\ 0.25,\ 0.275,\ 0.3,\ 0.325\ J_0$ have been used for room temperature.

Resulting absorption spectra $OD(\omega)$ and steady state fluorescence spectra $FL(\omega)$ averaged over 2000 realizations of Gaussian static disorder in transfer integrals δJ_{mn} for full Hamiltonian model and the nearest neighbour approximation one can be seen in Figure 2 (room temperature $kT = 0.5\ J_0$) and in Figure 3 (low temperature $kT = 0.1\ J_0$).

Peak position distributions of steady state fluorescence spectrum for single LH4 ring depend on the realization of static disorder and also on temperature. The resulting

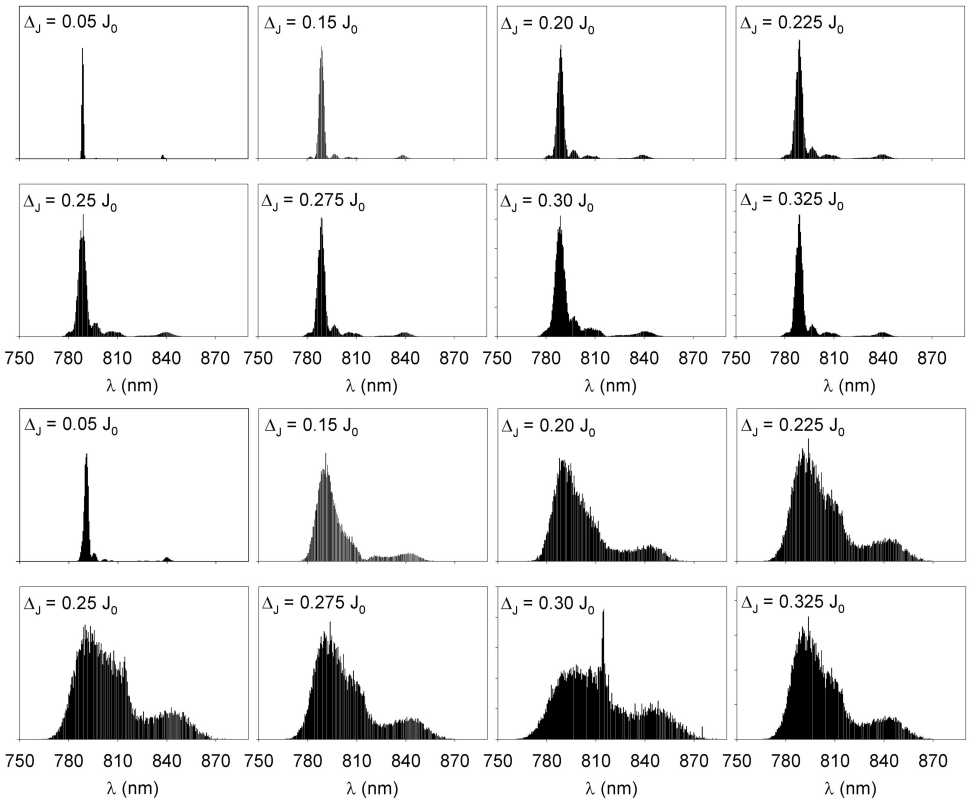

Fig. 6. The distributions of the quantity $P_\alpha d_\alpha^2$ as a function of wavelength λ at room temperature $kT = 0.5\ J_0$ for Gaussian uncorrelated static disorder in transfer integrals δJ_{mn} (eight strengths $\Delta_J = 0.05,\ 0.15,\ 0.20,\ 0.225,\ 0.25,\ 0.275,\ 0.30,\ 0.325\ J_0$, full Hamiltonian model – first and second row, the nearest neighbour approximation model – third and fourth row).

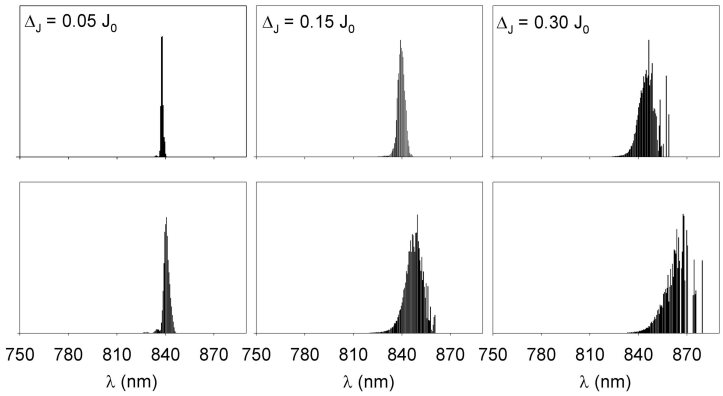

Fig. 7. The distributions of the quantity $P_\alpha d_\alpha^2$ as a function of wavelength λ at low temperature $kT = 0.1\ J_0$ for Gaussian uncorrelated static disorder in transfer integrals δJ_{mn} (three strengths $\Delta_J = 0.05,\ 0.15,\ 0.30\ J_0$, full Hamiltonian model – first row, the nearest neighbour approximation model – second row).

peak position distributions for both models are presented in Figure 4 (room temperature $kT = 0.5\ J_0$) and in Figure 5 (low temperature $kT = 0.1\ J_0$).

For clarification of fluorescence line splitting appearance in case of the nearest neighbour approximation model, the quantity $\sum_\alpha P_\alpha d_\alpha^2$ (see (12)) as a function of wavelength λ has been investigated. P_α is the steady state population of the eigenstate α, d_α^2 is the dipole strength of eigenstate α. The distributions of $P_\alpha d_\alpha^2$ as a function of wavelength λ, again for both models, for room temperature $kT = 0.5\ J_0$ and 2000 realizations of static disorder are presented in Figure 6 and for low temperature $kT = 0.1\ J_0$ in Figure 7.

The values of thermally averaged participation ratio $\langle PR \rangle$ for LH4 ring as a function of FL spectrum peak position calculated for 2000 realizations of above mentioned type of static disorder are shown in. Figure 8 (room temperature $kT = 0.5\ J_0$) and Figure 9 (low temperature $kT = 0.1\ J_0$).

V. Conclusions

Software package *Mathematica* has been found by us very useful for the simulations of the molecular ring spectra. From the comparison of our simulated $FL(\omega)$ and $OD(\omega)$ spectra for LH4 ring within full Hamiltonian model with our previous results calculated within the nearest neighbour approximation model (Figure 2, Figure 3, Figure 4, Figure 5) we can make following conclusions.

For low temperature $kT = 0.1\ J_0$ the absorption spectral line is wider in case of full Hamiltonian model in comparison with the nearest neighbour approximation model. For both models we can see the shift of the fluorescence spectral line to higher wavelengths (lower energies) for growing strength of static disorder. This shift is smaller for full Hamiltonian model as compared with the nearest neighbour approximation model. It is caused by the shift of energetic band to higher energies for full Hamiltonian model (see Figure 1).

For room temperature $kT = 0.5\ J_0$ the shift of fluorescence spectral line to higher wavelengths for growing strength of static disorder is visible in case of the nearest neighbour approximation model. In addition the splitting of fluorescence spectral line can be seen for $\Delta_J > 0.15\ J_0$ in case of this model. This effect is caused by different energetic band structures for both models (see Fig. 1). The optically active states in case of LH4 complex are the upper states $\alpha = \pm 7$ (unlike LH2 with lower optically active states $\alpha = \pm 1$). In case of room temperature upper states are more probably occupied and that is why the splitting can be seen only in case of room temperature (unlike LH2, where the splitting is visible only in case of low temperature and FH model). The absorption spectral line is wider for full Hamiltonian model. The reason of this effect is higher width of energetic band for this model in comparison with the nearest neighbour approximation model. Additionally, the absorption spectral line becomes narrower with growing strength of static disorder for the nearest neighbour approximation model. On the other hand only negligible changes of $FL(\omega)$ and $OD(\omega)$ spectral lines are distinguishable in case of the full Hamiltonian model for growing strength of static disorder.

As concern the peak position distributions (see Figure 4 and Figure 5), we can conclude that the distributions are significantly narrower for full Hamiltonian model in comparison with the nearest neighbour approximation model. In case of room temperature we can see the splitting of these distributions for the nearest neighbour approximation model. In case of low temperature any splitting of the peak position distributions is not visible and the distributions for full Hamiltonian model are significantly wider in comparison with room temperature. Similar conclusions can be made also from the distribu-

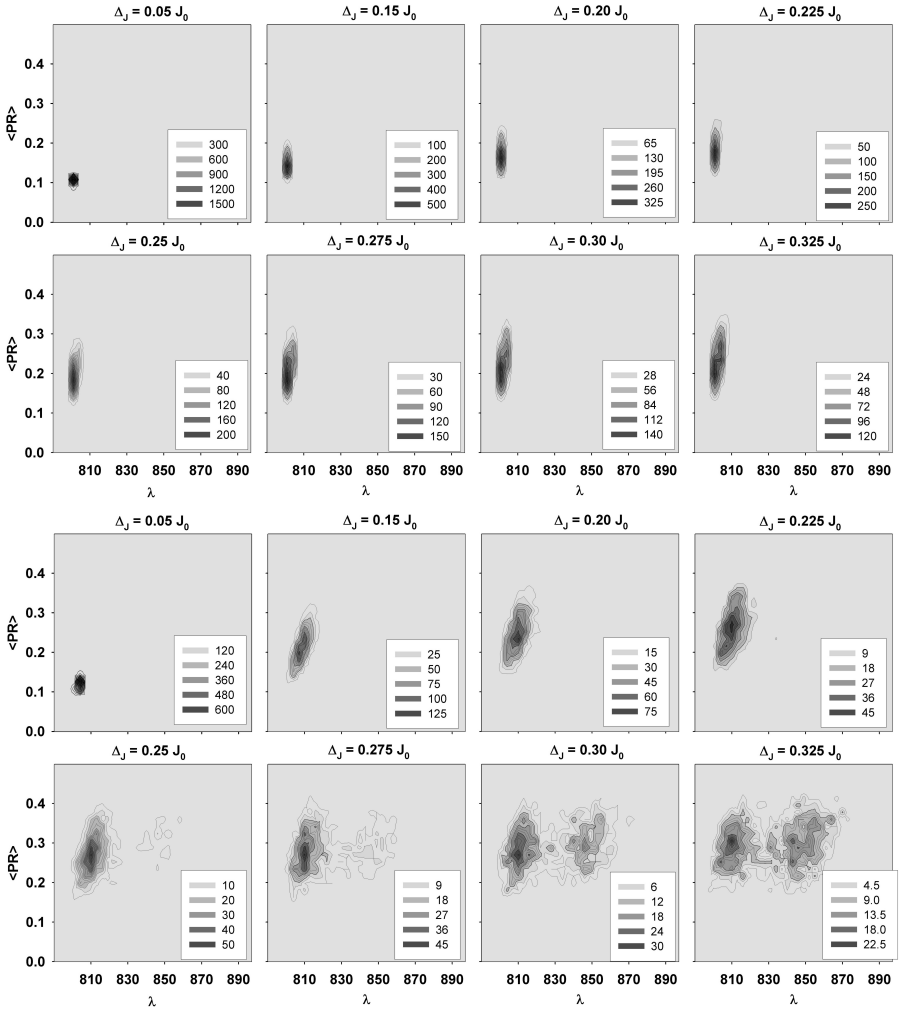

Fig. 8. The distribution of $\langle PR \rangle$ values of LH4 ring as a function of FL spectrum peak position at room temperature $kT = 0.5\ J_0$, calculated for 2000 realizations of Gaussian uncorrelated static disorder in transfer integrals δJ_{mn} (eight strengths $\Delta_J = 0.05,\ 0.15,\ 0.20,\ 0.225,\ 0.25,\ 0.275,\ 0.30,\ 0.325\ J_0$, full Hamiltonian model – first and second row, the nearest neighbour approximation model – third and fourth row).

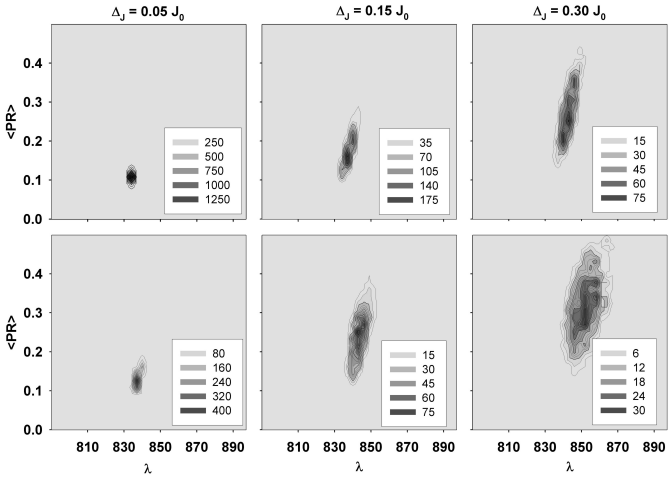

Fig. 9. The distribution of $\langle PR \rangle$ values of LH4 ring as a function of FL spectrum peak position at low temperature $kT = 0.1\ J_0$, calculated for 2000 realizations of Gaussian uncorrelated static disorder in transfer integrals δJ_{mn} (three strengths $\Delta_J = 0.05,\ 0.15,\ 0.30\ J_0$, full Hamiltonian model – first row, the nearest neighbour approximation model – second row).

tions of the quantity $P_\alpha d_\alpha^2$ (see Figure 6, Figure 7).

Substantial differences between above mentioned models are clear also in the distributions of $\langle PR \rangle$ values, especially for room temperature (see Figure 8 and Figure 9). The distributions are substantially wider and shifted to higher values of $\langle PR \rangle$ in case of the nearest neighbour approximation model. It corresponds to higher localization of exciton states in this model. Also the splitting of these distributions can be seen. Splitting of the peak position distributions, $P_\alpha d_\alpha^2$ distributions and $\langle PR \rangle$ values distributions for the nearest neighbour approximation model corresponds with the fluorescence spectral line splitting in this case.

REFERENCES

[1] R. van Grondelle, V. I. Novoderezhkin, Energy transfer in photosynthesis: experimental insights and quantitative models. *Physical Chemistry Chemical Physics* 8, 2003, pp. 793–807.

[2] A.W. Roszak et al., Crystal structure of the RC-LH1 core complex from Rhodopseudomonas palustris. *Science* 302, 2003, pp. 1976–1972.

[3] G. McDermott, S.M. Prince, A.A. Freer, A.M. Hawthornthwaite-Lawless, M.Z. Papiz, R.J. Cogdell, N.W. Isaacs, Crystal structure of an integral membrane light-harvesting complex from photosynthetic bacteria, *Nature* 374, 1995, pp. 517–521.

[4] M.Z. Papiz, S.M. Prince, T. Howard, R.J. Cogdell, N.W. Isaacs, The structure and thermal motion of the B 800850 LH2 complex from Rps. acidophila at 2.0 A resolution and 100 K: new structural features and functionally relevant motions, *J. Mol. Biol.* 326, 2003, pp. 1523–1538

[5] W.P.F. de Ruijter, et al., Observation of the Energy-Level Structure of the Low-Light Adapted B800 LH4 Complex by Single-Molecule Spectroscopy, *Biophys. J.* 87, 2004, pp. 3413–3420.

[6] R. Kumble, R. Hochstrasser, Disorder-induced exciton scattering in the light-harvesting systems of purple bacteria: Influence on the anisotropy of emission and band $\rightarrow$ band transitions, *J. Chem. Phys.* 109, 1998, pp. 855–865.

[7] V. Nagarajan et al., Ultrafast exciton relaxation in the B850 antenna complex of Rhodobacter sphaeroides, *Proc. Natl. Acad. Sci. USA* 93, 1996, pp. 13774–13779.

[8] V. Nagarajan et al., Femtosecond pump-probe spectroscopy of the B850 antenna complex of Rhodobacter sphaeroides at room temperature, *J. Phys. Chem. B* 103, 1999, pp. 2297–2309.

[9] V. Nagarajan, W. W. Parson, Femtosecond fluorescence depletion anisotropy: Application to the B850 antenna complex of Rhodobacter sphaeroides, *J. Phys. Chem. B* 104, 2000, pp. 4010–4013.

[10] V. Čápek, I. Barvík, P. Heřman, Towards proper parametrization in the exciton transfer and relaxation problem: dimer, *Chem. Phys.* 270, 2001, pp. 141–156.

[11] P. Heřman, I. Barvík, Towards proper parametrization in the exciton transfer and relaxation problem. II. Trimer, *Chem. Phys.* 274, 2001, pp. 199–217.

[12] P. Heřman, I. Barvík, M. Urbanec, Energy relaxation and transfer in excitonic trimer, *J. Lumin.* 108, 2004, pp. 85–89.

[13] P. Heřman et al., Exciton scattering in light-harvesting systems of purple bacteria, *J. Lumin.* 94-95, 2001, pp. 447–450.

[14] P. Heřman, I. Barvík, Non-Markovian effects in the anisotropy of emission in the ring antenna subunits of purple bacteria photosynthetic systems, *Czech. J. Phys.* 53, 2003, pp. 579–605.

[15] P. Heřman et al., Influence of static and dynamic disorder on the anisotropy of emission in the ring antenna subunits of purple bacteria photosynthetic systems, *Chem. Phys.* 275, 2002, pp. 1–13.

[16] P. Heřman, I. Barvík, Temperature dependence of the anisotropy of fluorescence in ring molecular systems, *J. Lumin.* 122–123, 2007, pp. 558–561.

[17] P. Heřman, I. Barvík, Coherence effects in ring molecular systems, *Phys. Stat. Sol. C* 3, 2006, 3408–3413.

[18] P. Heřman, D. Zapletal, I. Barvík, The anisotropy of fluorescence in ring units III: Tangential versus radial dipole arrangement, *J. Lumin.* 128, 2008, pp. 768–770.

[19] P. Heřman, I. Barvík, D. Zapletal, Computer simulation of the anisotropy of fluorescence in ring molecular systems: Tangential vs. radial dipole arrangement, *Lecture Notes in Computer Science* 5101, 2008, pp. 661–670.

[20] P. Heřman, D. Zapletal, J. Šlégr, Comparison of emission spectra of single LH2 complex for different types of disorder, *Phys. Proc.* 13, 2011, pp. 14–17.

[21] P. Heřman, D. Zapletal, M. Horák, Computer simulation of steady state emission and absorption spectra for molecular ring, *Proc. 5th International Conference on Advanced Engineering Computing and Applications in Sciences (ADVCOMP2011)*, Lisbon: IARIA, 2011, pp. 1–6.

[22] D. Zapletal, P. Heřman, Simulation of molecular ring emission spectra: localization of exciton states and dynamics. *Int. J. Math. Comp. Sim.* 6, 2012, pp. 144–152.

[23] M. Horák, P. Heřman, D. Zapletal, Simulation of molecular ring emission spectra - LH4 complex: localization of exciton states and dynamics. *Int. J. Math. Comp. Sim.* 7, 2013, pp. 85–93.

[24] M. Horák, P. Heřman, D. Zapletal, Modeling of emission spectra for molecular rings - LH2, LH4 complexes, *Phys. Proc.* 44, 2013, pp. 10–18.

[25] P. Heřman, D. Zapletal, Intermolecular coupling fluctuation effect on absorption and emission spectra for LH4 ring, *Int. J. Math. Comp. Sim.* 7, 2013, pp. 249–257.

[26] P. Heřman, D. Zapletal, M. Horák, Emission spectra of LH2 complex: full Hamiltonian model, *Eur. Phys. J. B* 86, 2013, art. no. 215.

[27] D. Zapletal, P. Heřman, Photosynthetic Complex LH2 - Absorption and Steady State Fluorescence Spectra, *Proc. of 6th Int. Conf. on Sust. Energy and Env. Protect. (SEEP2013)*, Maribor: University of Maribor, 2013, pp. 284–290.

[28] W. M. Zhang et al., Exciton-migration and three-pulse femtosecond optical spectroscopies of photosynthetic antenna complexes, *J. Chem. Phys.* 108, 1998, pp. 7763–7774.

[29] S. Mukamel, *Principles of nonlinear optical spectroscopy*. New York: Oxford University Press, 1995.

[30] A. G. Redfield, The Theory of Relaxation Processes, *Adv. Magn. Reson.* 1, 1965, pp. 1–32.

[31] D. Rutkauskas et al., Fluorescence spectroscopy of conformational changes of single LH2 complexes, *Biophys. J.* 88, 2005, pp. 422–435.

[32] D. Rutkauskas et al., Fluorescence spectral fluctuations of single LH2 complexes from *Rhodopseudomonas acidophila* strain 10050, *Biochemistry* 43, 2004, pp. 4431–4438.

[33] V. I. Novoderezhkin, D. Rutkauskas, R. van Grondelle, Dynamics of the emission spectrum of a single LH2 complex: Interplay of slow and fast nuclear motions, *Biophys. J.* 90, 2006, pp. 2890–2902.

[34] V. May, O. Kühn, *Charge and Energy Transfer in Molecular Systems*. Berlin: Wiley-WCH, 2000.

[35] O. Zerlauskiene et al., Static and Dynamic Protein Impact on Electronic Properties of Light-Harvesting Complex LH2, *J. Phys. Chem. B* 112, 2008, pp. 15883–15892.

[36] S. Wolfram, *The Mathematica Book*, 5th ed., Wolfram Media, 2003.

[37] M. Trott, *The Mathematica GuideBook for Symbolics*. New York: Springer Science+Business Media, Inc., 2006.

[38] M. Trott, *The Mathematica GuideBook for Numerics*. New York: Springer Science+Business Media, Inc., 2006.

[39] P. Heřman, D. Zapletal, I. Barvík, Lost of coherence due to disorder in molecular rings, *Phys. Stat. Sol. C* 6, 2009, 89–92.

[40] P. Heřman, I. Barvík, D. Zapletal, Energetic disorder and exciton states of individual molecular rings, *J. Lumin.* 119-120, 2006, pp. 496–503.